Nuclear Engineering and Technology 55 (2023) 1191–1198

Contents lists available at ScienceDirect

Nuclear Engineering and Technology

journal homepage: www.elsevier.com/locate/net

Technical Note

Investigation of the various properties of several candidate additives as buffer materials

Gi-Jun Lee [a], Seok Yoon [a, *], Taehyun Kim [b], Seeun Chang [a]

[a] Disposal Safety Evaluation Research Division, Korea Atomic Energy Research Institute (KAERI), Daejeon, 34057, South Korea
[b] Disposal Performance Demonstration on Research Division, Korea Atomic Energy Research Institute (KAERI), Daejeon, 34057, South Korea

ARTICLE INFO

Article history:
Received 4 August 2022
Received in revised form
21 November 2022
Accepted 21 November 2022
Available online 25 November 2022

Keywords:
Engineered barrier system
Bentonite buffer
Additives
THMC properties

ABSTRACT

Bentonite buffer material is a critical component in an engineered barrier system (EBS) for disposing high-level radioactive waste (HLW). The bentonite buffer material protects the disposal canister from groundwater penetration and releases decay heat to the surrounding rock mass; thus, it should possess high thermal conductivity, low hydraulic conductivity, and moderate swelling pressure to safely dispose the HLWs. Bentonite clay is a suitable buffer material because it satisfies the safety criteria. Several additives have been suggested as mixtures with bentonite to increase the thermal-hydraulic-mechanical-chemical (THMC) properties of bentonite buffer materials. Therefore, this study investigated the geotechnical, mineralogical, and THMC properties of several candidate additives such as sand, graphite, granite, and SiC powders. Datasets obtained in this study can be used to select adequate additives to improve the THMC properties of the buffer material.

1. Introduction

Nuclear fuel discarded after the operation of a nuclear power plant is called spent nuclear fuel. This fuel is a high-level waste (HLW) and it emits high decay heat and harmful radiation. Thus, a deep disposal system that comprises an artificially developed engineered barrier system (EBS) and a natural barrier system (NBS) is installed at a depth of 500–1000 m, as shown in Fig. 1 [1,2]. The EBS includes a disposal canister, bentonite buffer material, and backfill material. The design temperature of the bentonite buffer material is the most significant factor in the disposal system because it directly affects the disposal tunnel spacing and deposition hole spacing [3,4]. Most countries have limited the maximum operation temperature for bentonite buffer materials to 100 °C or less [4–6] because of its poor performance under long-term exposure to high temperatures. Thus, bentonites may not demonstrate required performances such as swellability owing to mineralogical deterioration. The distance between the disposal tunnel and deposition hole is within the range where the temperature of the buffer material does not exceed the maximum temperature. In Korea, the spacing of disposal tunnels is 40 m, and the spacing of deposition holes is 7.5 m based on the improved KAERI reference disposal system (KRS+) [7]. Research to reduce the required area of the HLW repository is essential because the area of the HLW repository required by the conditions of KRS+ is estimated to be several kilometers.

Several methods have been suggested to reduce the area of HLW repositories [1,2,8–10]. Further, studies have actively focused on developing enhanced buffer materials to improve the thermal-hydraulic-mechanical-chemical (THMC) performance of buffer materials by mixing various additives with existing bentonites [2,11–16]. Researchers investigated the thermal-hydraulic-mechanical properties of a buffer material by mixing graphite and sand with bentonite [11–16]. Zeng et al. [17] suggested a method of using claystone as an additive to recycle wastes from excavated rock where HLW repositories are constructed. The maximum temperature of the buffer material can be lowered by improving the thermal conductivity of the buffer material by mixing the additive with the existing bentonite, which helps decrease the spacing between the deposition hole and disposal tunnel [7,18]. Kim et al. [18] reported that the total disposal area can be reduced by approximately 40% if the thermal conductivity of the buffer material can be improved by 30% compared with that of the existing one.

Functional criteria of the buffer material are suggested for the safe operation of the HLW repository. Finland and Sweden are

* Corresponding author.
E-mail address: syoon@kaeri.re.kr (S. Yoon).

https://doi.org/10.1016/j.net.2022.11.017

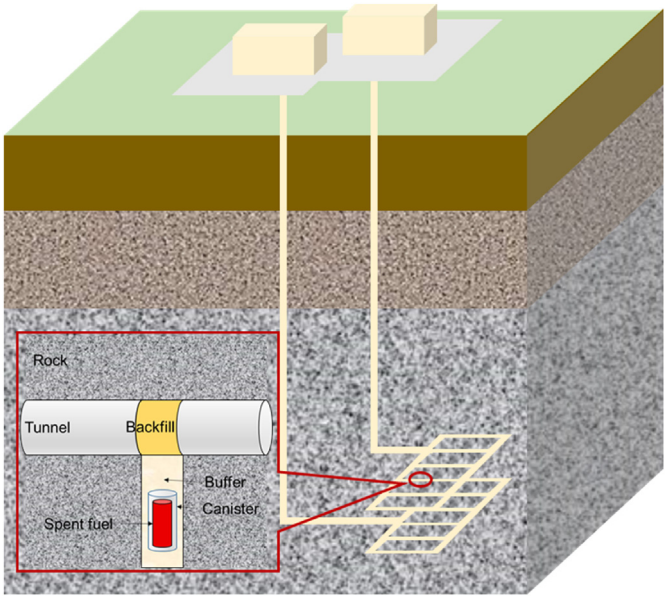

Fig. 1. Concept of EBS and NBS.

scheduled to operate the first repository in the world. They presented the functional criteria and design requirements of the buffer material, which are summarized in Tables 1 and 2, respectively. Therefore, research on the development of enhanced buffer materials that involves mixing bentonites with additives needs to be conducted for improving the functional criteria of the buffer materials presented in Table 1 [19] and 2 [19,20]. The buffer material must maintain its stability in the repository for hundreds of thousands of years. A natural material with very low organic carbon or sulfide content such as bentonite is suitable as a buffer material because organic matter acts as a nutrient for microorganisms, which produce sulfides that corrode the copper on the surface of the canister [20,21]. However, many studies have been conducted on the THMC characterization of buffer materials mixed with different additives and additive ratios [2,11–18], and data on the properties of the additive itself are insufficient to develop enhanced buffer materials that satisfy the functional criteria [19,20]. Therefore, additives suitable for long-term safety must be selected. Thus, the analyses of the specific gravity, specific surface area, particle size, constituent minerals, and constituent elements are required in addition to those of organic carbon and sulfide content. Further, THMC properties such as thermal conductivity, specific heat capacity, saturated hydraulic conductivity, swelling index, and nuclide sorption capacity, should be considered.

Among the materials with a stability and thermal conductivity higher than those of bentonite, granite powder, sand, and graphite powder are easily obtainable and have been used as additives for research on the development of enhanced buffer materials [12–16]. Furthermore, SiC significantly increases the thermal conductivity of inorganic matter [22]. Thus, granite powder, sand, graphite powder, and SiC were selected as additives in this study. Thus, the geotechnical, mineralogical, and THMC properties of granite powder, SiC, sand, and graphite were investigated in this study. The results with pure bentonite powder are compared and the suitability of the tested additives are discussed based on the datasets.

2. Analysis of basic properties of bentonite and various additives

Several tests were conducted to determine the basic properties of bentonite powder and the various additives. Specific gravity tests were conducted to determine the specific gravity of the sample, and sieve and laser-particle size tests were conducted to analyze the particle size distribution. The Brunauer–Emmett–Teller (BET) analysis was performed for the specific surface area, and the carbon (C) and sulfur (S) contents were analyzed. The analysis results are summarized in Table 3.

Gyeongju bentonite (KJ-2), which is a Ca-type bentonite, was used for the physical property tests. The location of the KJ-2 is presented in Fig. 2 which is from Google Earth [23]. KJ-2 has a specific gravity of 2.71, liquid limit of 146.7%, plasticity limit of 28.4%, and plasticity index of 118.3%, and it corresponds to CH based on the Unified Soil Classification system (USCS) [24, 25, Table 4]. The USCS is used to classify soil based on texture and grain size with soil plasticity.

The specific surface area is 61.5 m^2/g, which is significantly higher than the other additives in this research. The mean particle size (D_{50}) was 3.1 μm, and the 2 μm passing rate, which is a criterion to classify clay (<2 μm), is 48.4%. The total carbon and organic contents were 0.75% and 0.25%, respectively, and the S content was 0.30%. In addition, the basic properties of various additives including Jumunjin sand (Fig. 2), silica sand, graphite powder, and SiC powder were investigated; the results are summarized in Table 3. Besides SiC, which had a specific gravity of 3.2, the specific gravities of the other additives were similar. The D_{50} of the graphite and granite powders were similar, and the S contents of the additives ranged from less than 0.001 to 0.07.

3. Analysis of the composition of bentonite and various additives

X-ray diffraction (XRD) was performed to analyze the constituent minerals of the samples (Table 5). KJ-2 comprised 61.9% montmorillonite, 20.9% albite, 7.4% calcite, 5.3% quartz, 4.1% cristobalite, and 3.0% heulandite. Jumunjin sand contained 70.3% quartz, 23.6% microcline, and a small amount of muscovite. Silica sand comprised almost 100% quartz with small amounts of albite and muscovite, and the graphite powder was 100% graphite as a single component. The granite powder had 52% albite, 32.3% quartz, 9.1% biotite, 4.7% orthoclase, and 1.9% chlorite. The SiC powder contains 59.8% SiC (moissanite-6H), 39.4% SiC (moissanite-4H), 0.4% Si, and 0.3% graphite.

A series of X-ray fluorescence (XRF) analyses were performed

Table 1
Performance target of the buffer [19].

Performance target	Criteria	Safety function
Hydraulic conductivity	$<10^{-12}$ m/s	Limit advective mass transfer
Swelling pressure	>1 MPa	Limit advective mass transfer
	>2 MPa	Limit microbial activity
	<10 MPa	Protect the canister from detrimental mechanical load
	>0.2 MPa	Keep the canister in position
Temperature	<100 °C	Resist transformation

Table 2
Content of impurities [19,20].

Design parameter	Accepted variation (%)	Safety function
Total sulfur content (including sulphide)	<1	Compatibility and reliability of production (chemically favorable condition)
Sulphide content	<0.5	
Organic content	<1	

Table 3
Basic properties of the samples.

	KJ-II	Jumunjin sand	Silica sand	Graphite (powder)	Granite (powder)	SiC (powder)
Specific gravity	2.71	2.69	2.69	N/A	2.68	3.272
Liquid limit (%)	146.7	N/A	N/A	N/A	N/A	N/A
Plastic limit (%)	28.4	N/A	N/A	N/A	N/A	N/A
Plastic index (%)	118.3	N/A	N/A	N/A	N/A	N/A
USCS	CH	SP	SP	N/A	N/A	SP
Initial water content (%)	11–12	0	0	0	0	0
Specific surface (m^2/g)	61.5	0.2802	0.0418	8.6887	1.1961	0.0834
D_{50} (μm)	3.1	540	170–200	16.877	14.56	90
2 μm passing rate (%)	48.4	0	0	4	12.5	2.8
C content (Organic carbon) (%)	0.75 (0.25)	0.04	0.02	100	0.06	28.3
S content (%)	0.3	<0.001	<0.001	<0.001	0.07	0.01

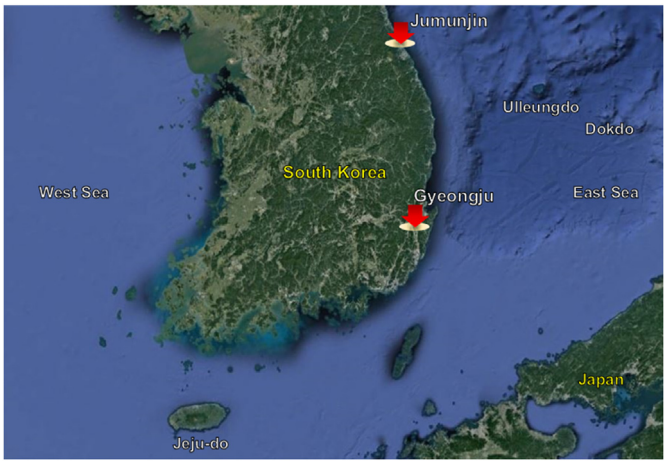

Fig. 2. Location of Gyeongju and Jumunjin, the origin of KJ-2 and Jumunjin sand taken from Google Earth [23].

for the qualitative and quantitative investigations of the constituent elements of each sample (Table 6). As summarized in Table 6, KJ-2 contains approximately five times more Ca cations than Na cations, and therefore, the XRF analysis confirmed that KJ-2 is a Ca-type bentonite. Jumunjin sand had 88.21% SiO_2 because the main constituent mineral was quartz, and this was followed by 6.31% Al_2O_3; each of the other elements contained less than 1%. Silica sand is composed of nearly 100% quartz, and therefore, the SiO_2 content was 98.41%; all other components were less than 1%. For graphite powder, the XRF result showed that ignition loss (Ig.loss)—the amount lost in baking a sample at a high temperature to remove impurities from the sample—existed because graphite powder consists of only carbon. Granite powder has 68.65% SiO_2, followed by 15.54% Al_2O_3, 3.89% Na_2O, 3.66% CaO, 2.95% Fe_2O_3, 2.04% K_2O, and 1.01% Ig.loss; all other elements were less than 1%.

4. Analysis of the THMC properties of bentonite and various additives

Various tests were performed for each characteristic to analyze the THMC properties of bentonite and the additives; the results are summarized in Table 7. Standard errors for thermal conductivity and hydraulic conductivity were calculated using the following equation.

$$Standard\ error = s/\sqrt{n} \quad (1)$$

where, s is standard deviation, and n is sample size. The standard errors of thermal conductivity and hydraulic conductivity were

Table 4
Unified soil classification system (USCS) from ASTM D2478-11 [24,25].

Major division	USCS group symbol	Typical description
Fine grained soils:~ clays and silts >50% (by weight) passing the 75 μm (#200) sieve	CH	High-plasticity clay
	CL	Low-plasticity clay
	MH	High-plasticity silt
	ML	Low-plasticity silt
Coarse grained soils:~ sands and gravels may contain up to 49% silt and clay >50% (by weight) coarser than 75 μm (#200) sieve	SC	Clayey sands
	SM	Silty sands
	SW	Clean sand-well graded
	SP	Clean sand-poorly graded
	GC	Clayey gravel, sand-clay-gravel
	GM	Silty gravel, gravel-sand-silt
	GW	Clean gravel-well graded
	GP	Clean gravel-poorly graded

Table 5
XRD analysis results of the samples (The units are in percentage).

Mineral	KJ-II	Jumunjin sand	Silica sand	Graphite (powder)	Granite (powder)	SiC (powder)
Montmorillonite	61.9	0	0	0	0	0
Albite	20.9	6.1	Tr	0	52	0
Quartz	5.3	70.3	100	0	32.3	0
Cristobalite	4.1	0	0	0	0	0
Calcite	7.4	0	0	0	0	0
Heulandite	3	0	0	0	0	0
Muscovite	0	Tr	Tr	0	0	0
Microcline	0	23.6	0	0	0	0
Biotite	0	Tr	0	0	9.1	0
Orthoclase	0	0	0	0	4.7	0
Chlorite	0	0	0	0	1.9	0
Graphite	0	0	0	100	0	0.3
Si	0	0	0	0	0	0.4
SiC(Moissanite-6H)	0	0	0	0	0	59.8
SiC(Moissanite-4H)	0	0	0	0	0	39.4

Table 6
XRF analysis results of the samples.

Chemical constituent (%)	SiO_2	Al_2O_3	Fe_2O_3	CaO	MgO	K_2O	Na_2O	TiO_2	MnO	P_2O_5	Ig. Loss
KJ-2	58.81	15.17	5.28	5.72	2.70	1.27	1.06	0.67	0.13	0	0
Jumunjin sand	88.21	6.31	0.25	0.11	0.05	0.39	0.68	0.07	<0.01	0.02	0.26
Silica sand	98.41	0.81	0.13	0.04	0.02	0.22	0.03	0.03	<0.01	0.01	0.23
Graphite (powder)	0.58	<0.01	1.62	<0.01	<0.01	<0.01	<0.02	<0.01	<0.01	<0.01	96.93
Granite (powder)	68.65	15.54	2.95	3.66	0.72	2.04	3.89	0.39	0.06	0.13	1.01

Table 7
THMC analysis results of the samples.

	Dry density (g/cm^3)	Thermal conductivity (W/(m·K)) /(Standard error)	Specific heat (kJ/kg·K)	D_{max}	D_{min}	Hydraulic conductivity (m/s)/ (Standard error)	Swelling Index (ml/2 g)	Relative density (%)	K_d (Cs, mL/g)	K_d (I, mL/g)
KJ-2	0.98	0.092–0.099 /(± 0.0035)	0.873–0.877	N/A	N/A	4–6x10^{-13} (γ_d:1.46 g/cm^3)/ (None)	6.5	N/A	682.37	0
	0.89	0.085 /(± 0.0035)	0.919			3.50 × 10^{-13} (γ_d:1.6 g/cm^3)/(± 12%)				
Jumunjin sand	1.53	0.211–0.22 /(± 0.004)	0.746–0.748	1.582*	1.411	3.29 × 10^{-7} (γ_d:1.58 g/cm^3)/ (None)	1.4–1.5	72	0	0
Silica sand	1.55	0.23–0.237 /(± 0.0035)	0.680–0.715	1.614	1.489	2.99 × 10^{-7} (γ_d:1.58 g/cm^3)/ (None)	1.5	51	6.9	0
Graphite (powder)	0.55	0.51 /(± 0.004)	0.752–0.755	N/A	N/A	5.88 × 10^{-7} (γ_d:0.44 g/cm^3)/(± 12%)	N/A	N/A	9.62	0
Granite (powder)	1.41	0.171 /(± 0.0035)	0.923	N/A	N/A	1.1 × 10^{-8} (γ_d:1.37 g/cm^3)/(None)	1.4	N/A	6.56	0.24
SiC	1.56	0.21 /(± 0.0035)	0.97	1.716	1.265	2.95 × 10^{-7} (γ_d:1.713 g/cm^3)/ (None)	0.86	72	0.33	0

Note: *Song et al., 2010.

within ± 3% and ± 12% of the measured value, respectively. For the rest of the samples except for the KJ-2 and the graphite powder, the hydraulic conductivity could not be measured several times, so the standard error could not be calculated for the samples except for the KJ-2 and the graphite powder. Considering that the standard error decreases as the n increases, and the low value of hydraulic conductivity, the measured values are reliable.

4.1. Thermal properties

Thermal conductivity was measured using KD2-Pro equipment, which uses a probe-type bar sensor inserted into a sample (Fig. 3). Before measuring the thermal properties of the samples, the thermal properties of a reference sample were measured, and the thermal conductivity of the silicon-epoxy reference sample was measured five times. The thermal conductivities were measured as 1.090, 1.027, 1.111, 1.098, and 1.091 W/(m·K) with deviations less than 6% and within 1.076 W/(m·K) (±10%). Thus, reliable measurements are possible. The degree of compaction of the sample is

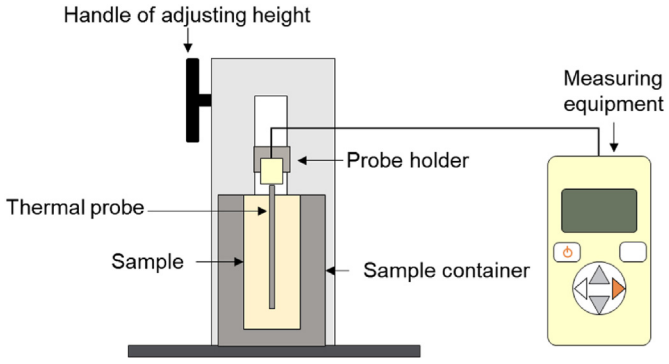

Fig. 3. Schematic of thermal conductivity test.

important because thermal conductivity depends on the dry density of the sample. The degree of compaction depends on the tester, and therefore, relative density is widely used to classify the degree of compaction in soil mechanics (26, 27, Table 8). The relative density (D_r) is defined by the maximum and minimum dry densities (γ_{dmax} and γ_{dmin}), as shown in.

$$D_r = \frac{\gamma_d - \gamma_{dmin}}{\gamma_{dmax} - \gamma_{dmin}} \cdot \frac{\gamma_{dmax}}{\gamma_d}. \quad (2)$$

Thus, the dry density (γ_d) of the sand and SiC samples in the maximum compaction and the minimum dry density in free fall were investigated. Finally, the relative density was calculated to investigate the sample compaction.

Fig. 4 shows thermal conductivities of the samples with dry densities. For KJ-2, the thermal conductivity was 0.085 and 0.092–0.099 W/(m·K), respectively, when the dry density was 0.89 and 0.98 g/cm^3; the specific heat at this condition were 0.919 and 0.873–0.877 kJ/(kg·K), respectively. The thermal properties of the additives were measured. For sand, the dry densities of Jumunjin and silica sands with different particle sizes were 1.53 and 1.55 g/cm^3, respectively; however, the relative density of Jumunjin sand was higher than that of silica sand, which implies that silica sand has more potential to increase thermal conductivity through compaction than Jumunjin sand. The thermal conductivity of SiC powder is like that of sand. SiC has high thermal conductivity; however, it corresponds to a high-temperature heat-treated SiC or a single crystal of pure SiC [28]. The SiC powder used in this study was nonpure SiC, not heat-treated, and it had an impurity lattice among the particles. Therefore, the structural defects of the SiC powder affected the thermal conductivity in this study [28].

In a previous study [29], the thermal conductivity of graphite powder was found to be approximately 130 W/(m·K). The equipment used for the thermal conductivity measurement in this study was available in the range of 0.1–4.0 W/(m·K). Therefore, the thermal conductivity of graphite powder at a low dry density of 0.55 g/cm^3 was measured as 0.51 W/(m·K). Although the powder had only a third of the dry density of the other additive samples, its thermal conductivity was the highest, more than twice that of the silica sand with a dry density of 1.55 g/cm^3. Table 9 shows the thermal conductivities of a 97 wt.% bentonite-3 wt.% graphite mixture from a preliminary test.

4.2. Hydraulic conductivity

A series of hydraulic conductivity tests were performed to measure the hydraulic conductivity of bentonite and the various additives used in this study. In the test, the dry sample is placed in a circular ring with a 50 mm diameter and 10 mm depth (Fig. 5). After placing the sample in the cell, different constant pressures were applied at the bottom and top of the sample using pressure pumps. A base pressure pump injected water at the bottom of the sample, and a back-pressure pump received water from the top of the sample. The pressure difference (hydraulic gradient) value between the top and bottom is determined and the hydraulic conductivity of the sample is calculated based on Darcy's law.

$$Q = K \cdot i \cdot A, \quad (3)$$

where Q, K, i, and A represent the flow rate (m^3/s), hydraulic conductivity (m/s), hydraulic gradient (m/m), and cross-sectional area of flow (m^2), respectively. Further, i is represented by the distance L (m) and hydraulic head difference Δh as

$$Q = K \cdot \Delta h / L \cdot A \quad (4)$$

Thus, the hydraulic conductivity can be calculated as

$$K = (Q \cdot L)/(\Delta h \cdot A) \quad (5)$$

For the KJ-2 sample, the pressure difference between the top and bottom of the sample was maintained at 1 MPa. The measured hydraulic conductivity value was small (3.50×10^{-13} m/s) when the dry density of the sample was 1.6 g/cm^3 because of the swellability and low void ratio of clay.

Hydraulic conductivities of the Jumunjin and silica sands were 3.29×10^{-7} m/s and 2.99×10^{-7} m/s, respectively (Fig. 6). For granite powder, hydraulic conductivity was 1.1×10^{-8} m/s. For graphite powder, the hydraulic conductivity is 5.88×10^{-7} m/s when the dry density is 0.44 g/cm^3. A comparison of the graphite and granite powders indicates that the hydraulic conductivity of graphite powder (5.88×10^{-7} m/s) is higher than that of granite powder (1.1×10^{-8} m/s) because of the lower dry density of graphite powder (0.44 g/cm^3). Further, when considering the same dry density condition, the hydraulic conductivity of the graphite powder is considered low because of its hydrophobicity. Therefore, the water passes through the graphite particles [30]. For the SiC powder, the hydraulic conductivity was 2.95×10^{-7} m/s. Considering the dry density of SiC powder (1.713 g/cm^3) at the measured hydraulic conductivity, the hydraulic conductivity was higher than that of sand because of the higher specific gravity of SiC (3.272) than that of sand (2.69).

4.3. Swelling index

The swelling index quantitatively indicates the swelling ability of a sample. A series of swelling index tests based on the ASTM D 5890 standard testing method were performed [31]. The first step in ASTM D 5890 is adding 0.1 g of the dried sample to a mass cylinder filled with 90 mL of distilled water at 10 min intervals for a total of 2 g. Then, additional distilled water was added to the mass cylinder to adjust to the 100 mL scale of the mass cylinder. After sealing the mass cylinder for 16 h, the swelling index was investigated as a sample volume of 2 g and checked the scale of the mass cylinder. The results indicate the swelling indices of the KJ-2, Jumunjin sand, silica sand, granite powder, and SiC powder were 6.5, 1.4–1.5, 1.5, 1.4, and 0.86 ml/2 g, respectively. Except for the KJ-2 bentonite, the other additives do not have the actual swelling ability, and therefore, the swelling indices of the sand and powder were considered to be the volume of the particles. The specific gravity of the SiC powder was the highest among the samples used in this study; the volume of 2 g was the smallest.

4.4. Sorption distribution coefficient

One of the functions of the buffer material is to prevent leakage of the nuclides; therefore, the sorption distribution coefficient of the enhanced buffer materials for nuclides must be large. The representative nuclides in this study were cesium and iodide ions, and their sorption distribution coefficients were measured. Thus,

Table 8
Compactness according to the relative density [26,27].

Relative density (%)	Compactness
0–15	Very loose
15–35	Loose
35–65	Medium
65–85	Dense
85–100	Very dense

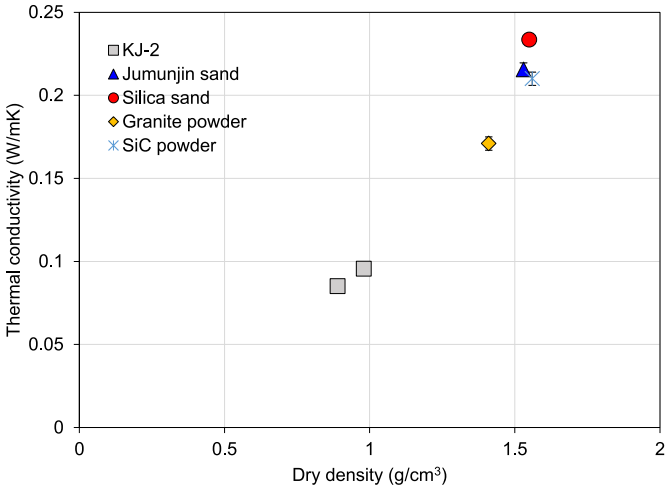

Fig. 4. Thermal conductivity of samples with dry density.

batch sorption experiments were conducted on bentonite and additives in contact with cesium- and iodide-spiked water. Cesium chloride (CsCl) and sodium iodide (NaI) were used as reagent grade (>99.5%, Sigma-Aldrich) chemicals to prepare the desired solutions (both 100 mg/L) without any purification. The cesium and iodide ions (Cs^+ and I^-) were dissolved in deionized water (18 MΩ water, Young In Chromass, Aquapuri 541, Korea), respectively. The experiments were conducted in individual 50 mL polypropylene centrifuge tubes by mixing sorbents (bentonite and additives) with no pretreatment and solutions, and by placing the tubes on a platform shaker at 150 rpm. A 10-day equilibration time was considered sufficient to reach the steady state [32–34]. The solid-solution ratio was 1:100 (0.4 g/40 mL) for the batch experiments. A control sample of the solution with no sorbent was prepared in an identical manner to determine any sorption to the test centrifuge tubes. After 10 days of mixing, the suspensions were centrifuged at 3000 rpm and the supernatants were filtered using 0.45 μm PVDF filters. The initial and final concentrations of Cs^+ and I^- were measured by ICP-OES (Varian, ICP-730ES, Australia) and ICP-MS (PerkinElmer, NexION 300S, USA), respectively. Although I^- is a volatile ion, no chemical substance was added because no analysis error could be attributed to volatilization. All batch sorption experiments were performed under aerobic conditions at room temperature and in duplicate for all experimental conditions. The sorption distribution coefficient, K_d (mL/g), represents the solute concentration sorbed onto the sorbent; it was calculated using the difference between the initial and equilibrium concentrations after the reaction. The equation is expressed as [34].

$$K_d = \frac{(C_o - C_q)}{C_q} \cdot \frac{V}{M}, \tag{6}$$

where C_o and C_q (mg/L) represent the initial and equilibrium concentrations in the solution, respectively, V (mL) represents the solution volume, and M represents the solid mass (g). The control test value was not considered to calculate K_d because the amount sorbed on the test tubes was negligible.

5. Discussions

The basic properties, including the specific gravity, particle size, organic content, and mineral and chemical composition of the additives used in this study were investigated because the THMC properties of the additives affected the performance of the buffer material. Measured data were used to analyze the effects of the investigated properties on the THMC properties, including the dry density and thermal and hydraulic conductivity.

5.1. Effects of basic properties on THMC properties in the additives

The basic properties examined in this study were specific

Table 9
Thermal conductivity of block-type buffer materials.

Dry density (g/cm³)	Water content (%)	Bentonite (KJ-2) ratio (wt.%)	Graphite powder ratio (wt.%)	Thermal conductivity (W/(m·K))
1.6	12	100	0	0.84
1.51	12.3	97	3	0.95

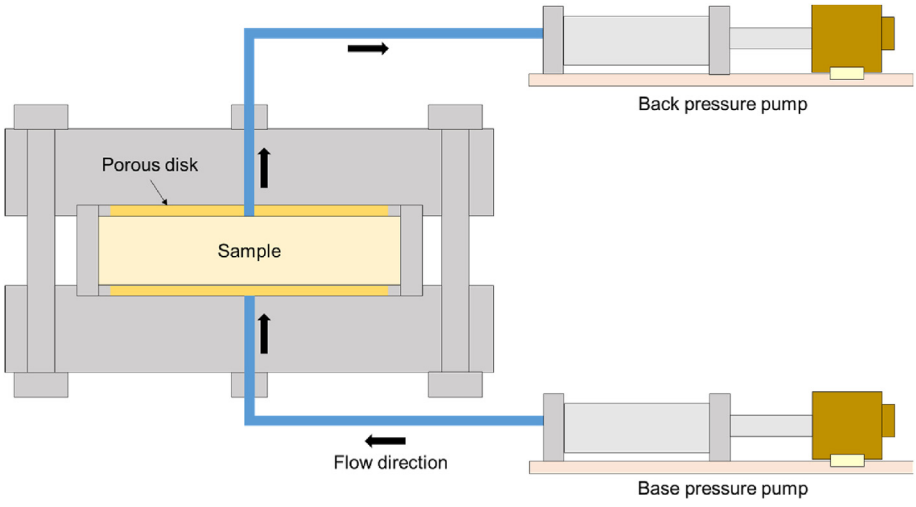

Fig. 5. Schematic of the hydraulic conductivity test.

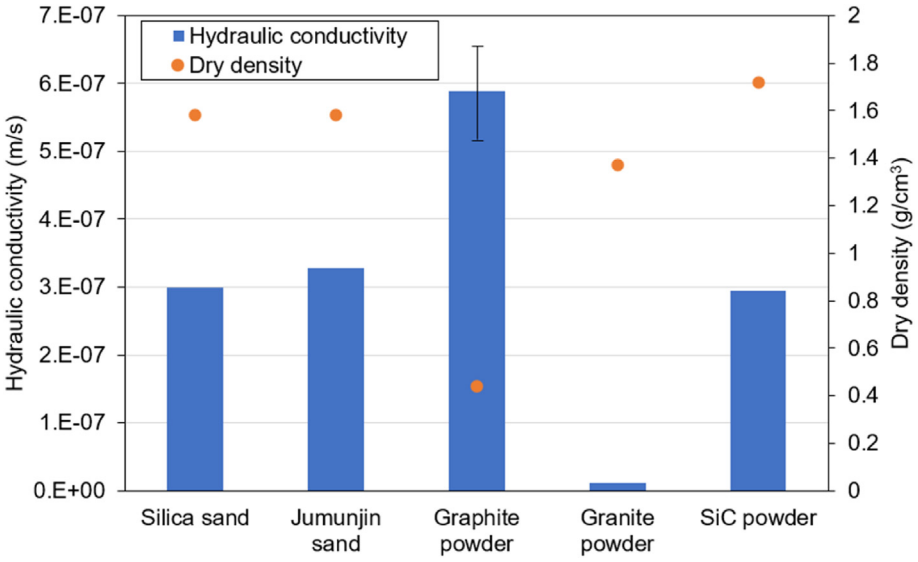

Fig. 6. Hydraulic conductivity of the samples.

gravity, particle size, carbon, and sulfide content (Table 3). Among these basic properties, the specific gravities of the KJ-2 and the sand samples did not show considerable difference. However, the specific gravity of SiC was 3.272, which was 20.7% higher than that of the KJ-2. A higher dry density results in a lower void ratio in the samples; hence, there is an increase in the thermal conductivity. However, in the case of additives with higher specific gravity, such as SiC, the dry density may not be an appropriate parameter for examining the thermal conductivity. For SiC, the total added SiC volume in the buffer material could be too small owing to the high specific gravity when considering the same dry density condition as the other additives. A lower added SiC volume in the buffer material could cause a decrease in the thermal conductivity because of the lower void ratio. Therefore, it may be appropriate to examine the change in thermal conductivity according to the same additive volume, rather than the dry density for additives with a large specific gravity, such as SiC.

KJ-2 showed the largest specific surface area. Among the additives, graphite powder had the largest specific surface area (8.6887 m^2/g); the thermal conductivity of graphite powder was the highest among the additives. Granite powder has a specific surface area approximately five times larger than that of Jumunjin sand. A larger specific surface area results in a larger contact area between particles, and therefore, it can increase thermal conductivity. However, the thermal conductivities of the Jumunjin sand and granite powders do not show considerable difference under similar dry density conditions, even with five times the higher specific surface area of the granite powder. In addition, the same tendency was observed when comparing the Jumunjin and silica sands. Therefore, a large specific surface area is not necessarily superior to thermal conductivity.

Moreover, the effect of particle size on the THMC properties was investigated. The void ratio is closely related to the particle size, and therefore, the thermal and hydraulic conductivities may be affected by particle size. The void ratio of a buffer material increases when an additive with a large particle size is used. However, the thermal conductivity of a buffer material can increase even with an increasing void ratio because the high thermal conductivity of an additive affects heat transfer. The thermal conductivity is reduced because of the excessive increase in the void ratio if the ratio of the large-particle additive exceeds a specific range [30]. However, hydraulic conductivity may increase with an increasing void ratio, as shown in this study (Table 6). Therefore, a powder-type additive with a fine grain size may be more suitable for enhancing buffer performance than sand when there is an increase in the mixing ratio of an additive.

5.2. Effects of mineral and chemical constituents on THMC properties in the additives

The effects of mineral and chemical constituents on the THMC properties of the additives were investigated. The thermal conductivity increases with a higher quartz ratio [35]; however, thermal conductivities of granite powder and sand did not show considerable differences under similar dry density conditions, even with a significant difference in the quartz content (Table 5). The XRF results were investigated to determine the cause of this unexpected tendency. The XRF results indicated that the SiO_2 content did not show considerable differences when comparing the sand and granite powders; further, the thermal conductivity showed a higher value in the order of the SiO_2 content (Table 6). Si is an element with high thermal conductivity [36], and minerals other than quartz in the XRD results may include Si. Therefore, evaluating the thermal conductivity based on the quartz and SiO_2 content might be appropriate.

6. Conclusions

In this study, additives were mixed with bentonite powder to improve its THMC properties for use as a buffer material and reduce the disposal area. The geotechnical, XRD, XRF, and THMC properties of several candidate additives were investigated. Two types of sand, graphite, granite, and SiC powders were tested and compared with bentonite powder; the following conclusions were obtained:

- There were few sulfides and organic carbon in each additive.
- A large specific surface area is not necessarily conducive to better thermal conductivity.
- Thermal conductivity should be judged by evaluating the SiO_2 content and not just the quartz content.
- The void ratio is closely related to the particle size; therefore, the thermal and hydraulic conductivities of bentonite

mixtures are affected by particle size. Thus, silica sand is more advantageous than Jumunjin sand in terms of thermal and hydraulic conductivities of mixtures.
- When the mixing ratio of an additive increases, an additive with a fine grain size, such as granite powder, might be more suitable than sand for buffer enhancement.
- Furthermore, granite powder adsorbs nuclides; thus, granite power is more advantageous than sand as an additive in terms of chemical aspects.
- Among the additives used in this study, silica sand, Jumunjin sand, graphite, granite, and SiC powders, graphite powder showed the highest efficiency in thermal conductivity.
- In the future, the change in thermal conductivity for additives with a large specific gravity, such as SiC, should be investigated according to the additive volume and not dry density.

Declaration of competing interest

The authors declare that they have no known competing financial interests or personal relationships that could have appeared to influence the work reported in this paper.

Acknowledgements

This research was funded by the Nuclear Research and Development Program (2021M2E3A2041351) by the National Research Foundation of Korea, and Institute for Korea Spent Nuclear Fuel and National Research Foundation of Korea (2021M2E1A1085193).

References

[1] W.J. Cho, J.O. Lee, S. Kwon, Analysis of thermos-hydro-mechanical process in the engineered barrier system of a high-level waste repository, Nucl. Eng. Des. 240 (2010) 1688–1698.
[2] Y.G. Chen, X.M.L. Liu, X. Mu, W.M. Ye, Y.J. Cui, B. Chen, D.B. Wu, Thermal conductivity of compacted GO-GMZ bentonite used as buffer material for a high-level radioactive waste repository, Adv. Civ. Eng. 2018 (9530813) (2018) 11.
[3] S. Yoon, G.J. Lee, T.J. Park, C. Lee, D.K. Cho, Thermal conductivity evaluation for bentonite buffer materials under elevated temperature conditions, Case Stud. Therm. Eng. 30 (2022), 101792.
[4] SKB, Design Premises for a KBS-3V Repository Based on Results from the Safety Assessment SR-Can and Some Subsequent Analyses, SKB TR-09-22, SKB, 2009.
[5] JNC, H12 Project to Establish the Scientific and Technical Basis for HLW Disposal in Japan (Supporting Report 2) Repository Design and Engineering Technology. JNC TN1410 2000-003, Japan Nuclear Cycle Development Institute, Tokai, Japan, 1999.
[6] G.R. Simmons, P. Baumgartner, The Disposal of Canada's Nuclear Fuel Waste: Engineering for a Disposal Facility, AECL-10715, Atomic Energy of Canada Limited, 1994.
[7] K.I. Kim, C. Lee, J. Lee, J.S. Kim, D.K. Cho, Estimation of Disposal Spacing and Rock Mass Conditions for High-Efficiency Repository Based on Temperature Limit Requirement of Bentonite Buffer, 2021. KAERI/TR-8711/2021.
[8] P. Wersin, L.H. Johnson, I.G. McKinley, Performance of the bentonite barrier at temperatures beyond 100 °C: a critical review, Phys. Chem. Earth 32 (2007) 780–788.
[9] L. Zhen, J. Rutqvist, J.T. Birkholzer, H. Liu, On the impact of temperatures up to 200 °C in clay repositories with bentonite engineer barrier systems: a study with coupled thermal, hydrological, chemical, and mechanical modeling, Eng. Geol. 197 (2015) 278–295.
[10] V.R. Ouhadi, R.N. Yong, A.R. Goodarzi, M. Safari-Zanjani, Effect of temperature on the re-structuring of microstructure and geo-environmental behavior of smectite, Appl. Clay Sci. 47 (2010) 2–9.
[11] F. Peng, Y. Tan, Thermal conductivity of bentonite-graphite mixture and its prediction for high-level radioactive waste repository, Ann. Nucl. Energy 154 (2021), 108142.
[12] L. Xu, W.M. Ye, B. Chen, Y.G. Chen, Y.J. Cui, Experimental investigations on thermo-hydro-mechanical properties of compacted GMZ01 bentonite-sand mixture using as buffer materials, Eng. Geol. 213 (2016) 46–54.
[13] Z.G. Chen, C.S. Tang, C. Zhu, B. Shi, Y.M. Liu, Compression, swelling and rebound behavior of GMZ bentonite/additive mixture under coupled hydro-mechanical condition, Eng. Geol. 221 (2017) 50–60.
[14] P.V. Sivapullaiah, A. Sridharan, V.K. Stalin, Hydraulic conductivity of bentonite-sand mixtures, Can. Geotech. J. 37 (2) (2000) 406–413.
[15] S. Saba, J.D. Barnichon, Y.J. Cui, A.M. Tang, P. Delage, Microstructure and anisotropic swelling behaviour of compacted bentonite/sand mixture, J. Rock Mech. Geotech. Eng. 6 (2) (2014) 126–132.
[16] X. Liu, G. Cai, L. Liu, S. Liu, A.J. Puppala, Thermo-hydro-mechanical properties of bentonite-sand-graphite-polypropylene fiber mixtures as buffer materials for a high-level radioactive waste repository, Int. J. Heat Mass Tran. 141 (2019) 981–994.
[17] Z. Zeng, Y.J. Cui, J. Talandier, An insight into grain interaction in bentonite/claystone mixture, Acta Geotechnica (2022) 1–7.
[18] M.J. Kim, G.J. Lee, S. Yoon, Numerical study on the effect of enhanced buffer materials in a high-level radioactive waste repository, Appl. Sci. 11 (18) (2021) 8733.
[19] Posiva SKB, Safety Functions, Performance Target and Technical Design Requirements for a KBS-3V Repository, Posiva SKB Report 01, Posiva Oy, 2017.
[20] M. Juvankoski, Buffer Design 2012, Posiva 2012-14, Posiva Oy, 2013.
[21] W.J. Cho, Bentonite Barrier Material for Radioactive Waste Disposal, 2019. KAERI/GP-535/2019.
[22] W.A. Nevin, H. Yamagishi, M. Yamaguchi, Y. Tawada, Emission of blue light from hydrogenated amorphous silicon carbide, Nature 368 (6471) (1994) 529–531.
[23] Google Earth, South Korea, https://earth.google.com/web/.
[24] ASTM, D2487-11 Standard Practice for Classification of Soils for Engineering Purposes (Unified Soil Classification System), ASTM International, West Conshohocken, 2011.
[25] S.N. Warren, R.R. Kallu, C.K. Barnard, Correlation of the rock mass rating (RMR) system with the unified soil classification system (USCS): introduction of the weak rock mass rating system (W-RMR), Rock Mech. Rock Eng. 49 (11) (2016) 4507–4518.
[26] S.R. Kaniraj, Design Aids in Soil Mechanics and Foundation Engineering, McGraw Hill Education (India) Private Limited, New Delhi, 1988.
[27] S. Roy, S.K. Bhalla, Role of geotechnical properties of soil on civil engineering structures, Resour. Environ. 7 (4) (2017) 103–109.
[28] Y. Zhou, K. Hirao, K. Watari, Y. Yamauchi, S. Kanzaki, Thermal conductivity of silicon carbide densified with rare-earth oxide additives, J. Eur. Ceram. Soc. 24 (2) (2004) 265–270.
[29] M. Lee, H.J. Choi, J.W. Lee, J.P. Lee, Improvement of the Thermal Conductivity of a Compact Bentonite Buffer, 2013. KAERI/TR-5311/2013.
[30] Y.Z. Tan, Z.Y. Xie, F. Peng, F.H. Qian, H.J. Ming, Optimal mixing scheme for graphite-bentonite mixtures used as buffer materials in high-level waste repositories, Environ. Earth Sci. 80 (17) (2021) 1–13.
[31] ASTM D5890-19, Standard Test Method for Swell Index of Clay Mineral Component of Geosynthetic Clay Liners, ASTM International, West Conshohocken, PA, 2019.
[32] T. Huitti, M. Hakanen, A. Lindberg, Sorption of Cesium on Olkiluoto Mica Gneiss, in: Granodiorite and Granite, Posiva, vols. 98–11, Posiva Oy, Helsinki, 1998.
[33] W. Um, R.J. Serne, C.F. Brown, G.V. Last, U(VI) adsorption on 200-UP-1 aquifer sediments at the Hanford Site, J. Contam. Hydrol. 93 (2007) 1.
[34] S. Chang, W. Um, W. Kim, H. Kim, Effect of seawater intrusion on radioactive strontium (90Sr) sorption and transport at nuclear power plants, Radiochim. Acta 106 (2018) 2.
[35] G.J. Lee, S. Yoon, W.J. Cho, Effect of bentonite type on thermal conductivity in a HLW repository, J. Nucl. Fuel Cycle Waste Technol. 19 (3) (2021) 331–338.
[36] P. Chantrenne, J.L. Barrat, X. Blase, J.D. Gale, An analytical model for the thermal conductivity of silicon nanostructures, J. Appl. Phys. 97 (10) (2005), 104318.